

# **Scalable all-polymer dielectric films with aligned structures for high-temperature energy storage applications**

Xin Zhen,<sup>a</sup> Jian Wang,<sup>a</sup> Xinhui Li,<sup>a</sup> Yanda Jiang,<sup>a</sup> Zhi Li,<sup>a</sup> Zhonghui Shen,<sup>a</sup> and Xin Zhang<sup>\*a</sup>

<sup>a</sup> State Key Laboratory of Advanced Technology for Materials Synthesis and Processing, Center of Smart Materials and Devices& International School of Materials Science and Engineering, Wuhan University of Technology, Wuhan 430070, China. E-mail: zhang-xin@whut.edu.cn

\*Corresponding authors  
E-mail: zhang-xin@whut.edu.cn

**Table. S1** Definition of parameters used in this simulation.

Parameter	Values	Units
Schottky barrier	1.25	eV
Trap depth	0.2	eV
Charge mobility of PEI	$1 \times 10^{-12}$	$\text{cm}^2/(\text{V}\cdot\text{s})$
Charge mobility of PVDF	$1 \times 10^{-8}$	$\text{cm}^2/(\text{V}\cdot\text{s})$
Electric field	100	MV/m
Temperature	423	K

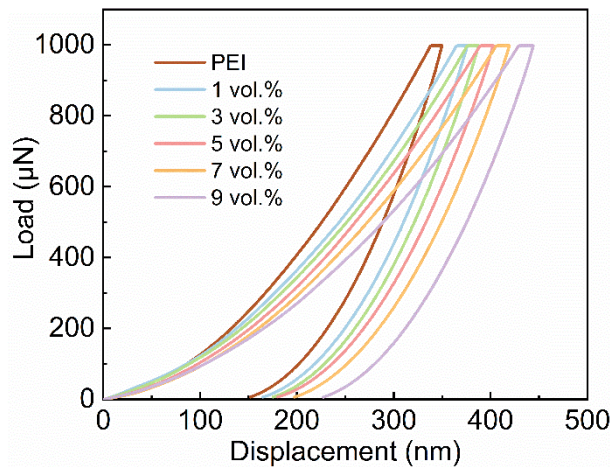


**Fig. S1** The load-displacement curves for all-organic composite films with different PEI/PVDF components.

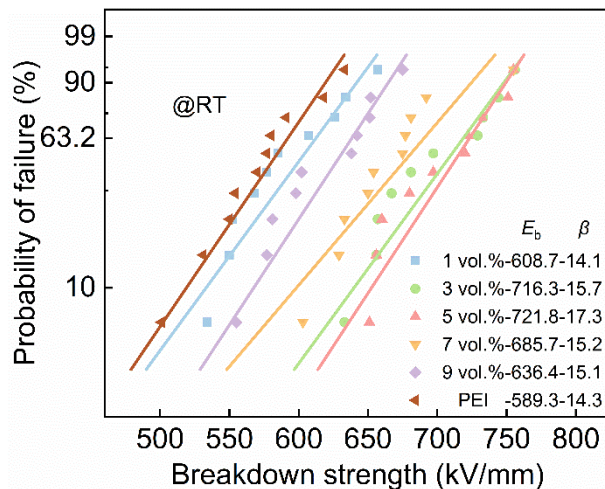


**Fig. S2** Weibull breakdown characteristics of all-organic composite films with different PEI/PVDF components at room temperature.

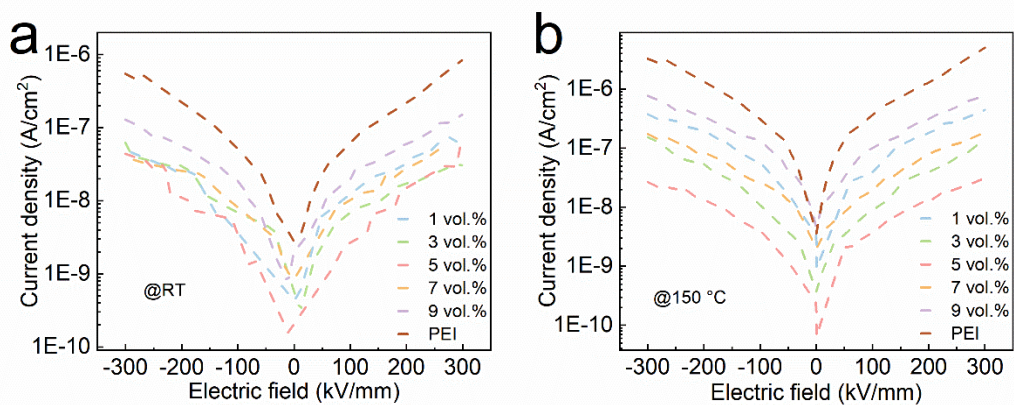


**Fig. S3** Variation of leakage current density with the applied electric field at a) room temperature and b) 150 °C.

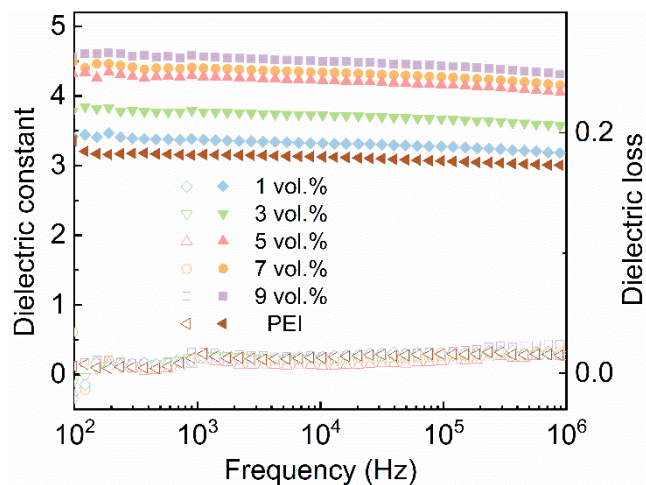


**Fig. S4** The dependence of dielectric constant-loss of all-organic composite films with different PEI/PVDF components on frequency.

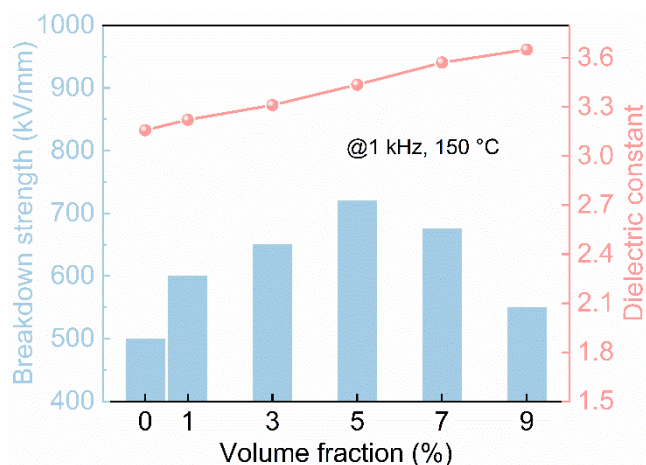


**Fig. S5** Variation of dielectric constant and breakdown strength as a function of different PEI/PVDF components at 1 kHz and 150 °C.

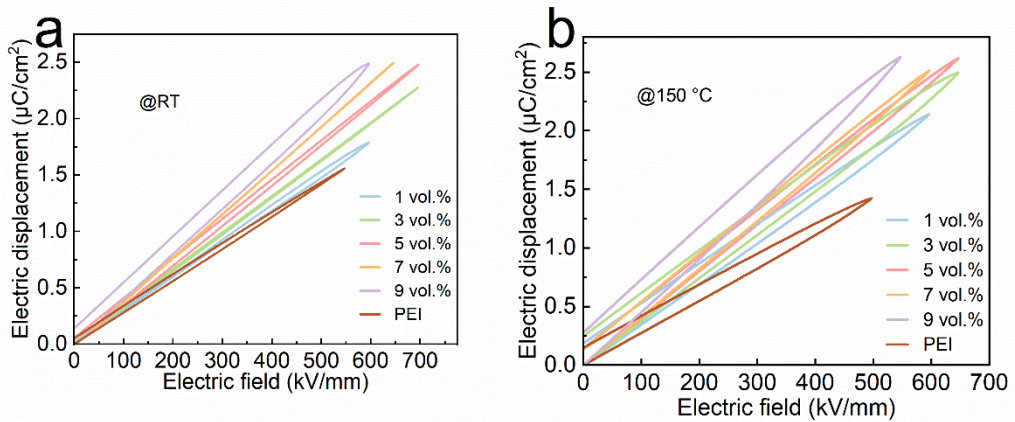


**Fig. S6**  $D$ - $E$  loops of all-organic composite films with different PEI/PVDF components at  
a) room temperature and b) 150 °C.

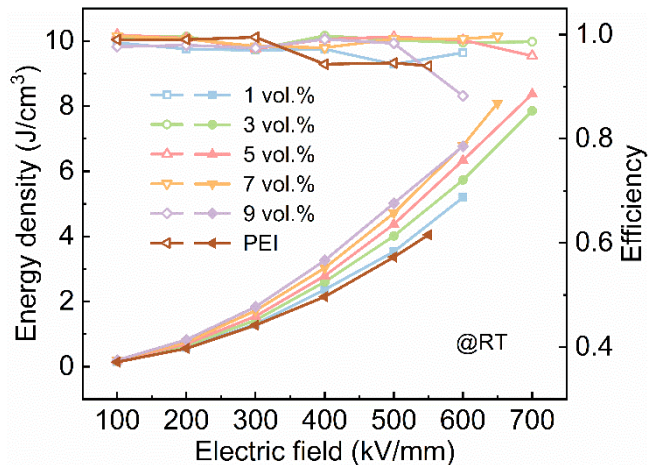


**Fig. S7** Variation of energy storage density and charge-discharge efficiency with the applied external electric field at room temperature.

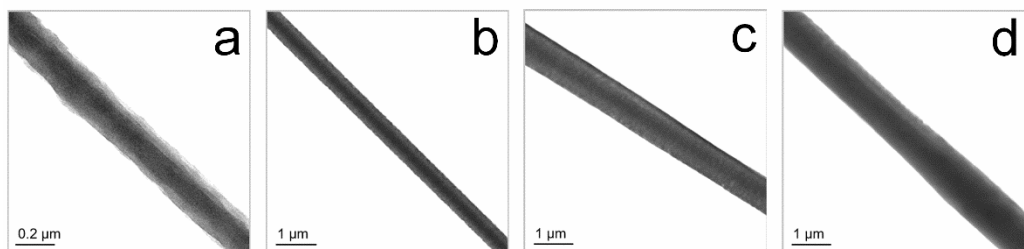


**Fig. S8** The SEM images with fibers of diameters a) 200 nm, b) 500 nm, c) 1  $\mu\text{m}$   
and d) 1.5  $\mu\text{m}$

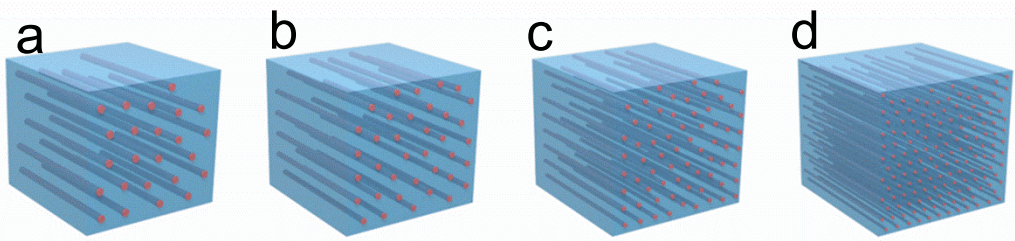


**Fig. S9** Schematic illustration of films with different fiber diameters a) 1.5  $\mu\text{m}$ , b) 1  $\mu\text{m}$ , c) 500 nm and d) 200 nm

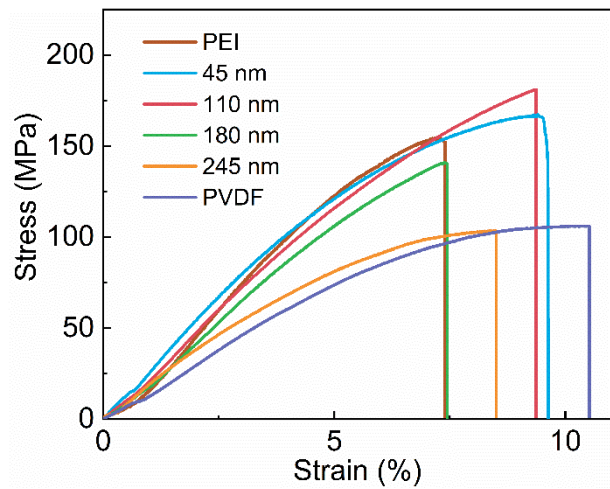


**Fig. S10** Stress-strain curves of composite films loaded with different fiber diameters of 5 vol.% PEI/PVDF

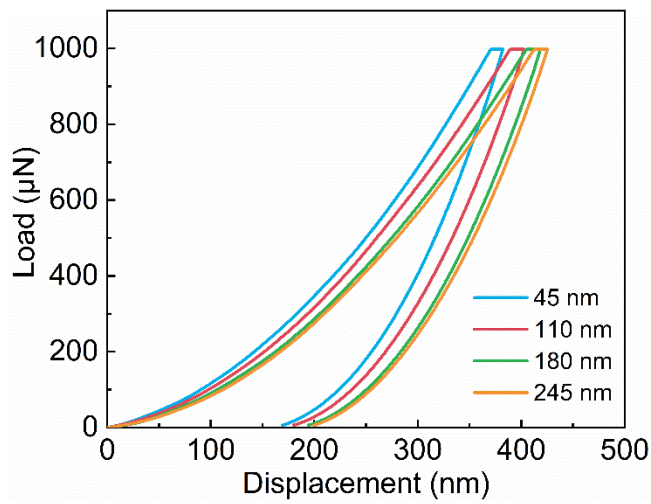


**Fig. S11** The load-displacement curves for different fiber diameters of 5 vol.% PEI/PVDF

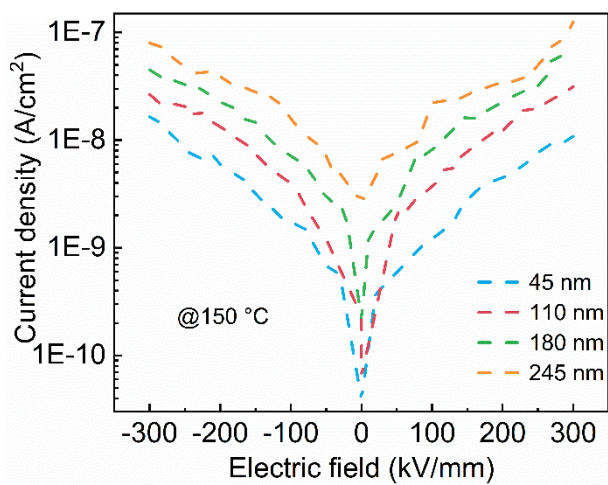


**Fig. S12** Variation of leakage current density with the applied electric field at 150 °C

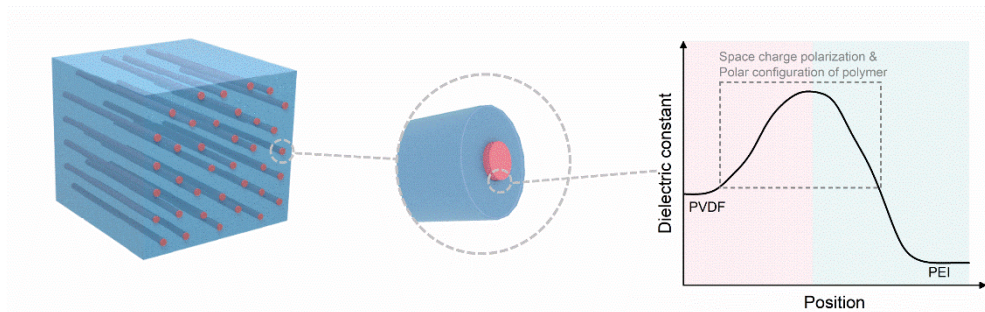


**Fig. S13** Schematic illustration of the interfacial polarization mechanism

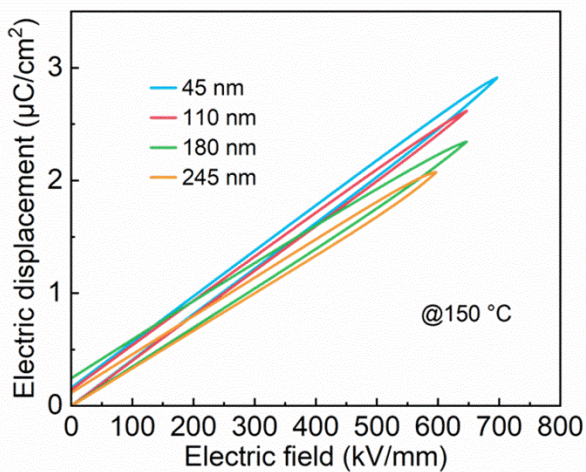


**Fig. S14**  $D$ - $E$  loops of films with different fiber diameters of 5 vol.% PEI/PVDF at 150 °C

**Table. S2** The dielectric and energy storage properties at 150 °C of previously published polymer-based dielectrics and the PEI/PVDF composite in this work.

Composites	$U_d$ (J/cm <sup>3</sup> )	$\eta$ (%)	$E_b$ (kV/mm)	$\epsilon_r$
PEI/PVDF (this work)	9.39	>90	711	4.44
PEI/PCBM <sup>1</sup>	4.5	>90	~550	~3.5
POFN <sup>2</sup>	5.7	~77	~686	2.5
ITIC/PEI <sup>3</sup>	6.37	>90	560	3.2
o-POFN <sup>4</sup>	8.3	~83	~800	~2.88
CS-ODA <sup>5</sup>	7.02	>90	641.7	3.53
PC-BN-SiO <sub>2</sub> <sup>6</sup>	5.22	~76	610	~3.0
PEI-Al <sub>2</sub> O <sub>3</sub> <sup>7</sup>	3.5	>90	636.4	~3.1
F-PI/PCBM <sup>8</sup>	6.39	>90	815	2.99
PI-PAA/BNNS <sup>9</sup>	7.4	~47	527	4.05
PEEU-Al <sub>2</sub> O <sub>3</sub> <sup>10</sup>	5	90	600	7.4
NTCDA/PEI <sup>11</sup>	5.1	90	630	~3.2
ITIC-PI@PEI <sup>12</sup>	4	~63	505	~3.27

## References

- 1 C. Yuan, Y. Zhou, Y. Zhu, J. Liang, S. Wang, S. Peng, Y. Li, S. Cheng, M. Yang, J. Hu, B. Zhang, R. Zeng, J. He and Q. Li, *Nat. Commun.*, 2020, **11**, 3919.
- 2 C. Wu, A. A. Deshmukh, Z. Li, L. Chen, A. Alamri, Y. Wang, R. Ramprasad, G. A. Sotzing and Y. Cao, *Adv. Mater.*, 2020, **32**, 2000499.
- 3 M. Feng, Y. Feng, C. Zhang, T. Zhang, Q. Chen and Q. Chi, *Mater. Horiz.*, 2022, **9**, 3002–3012.
- 4 A. A. Deshmukh, C. Wu, O. Yassin, A. Mishra, L. Chen, A. Alamri, Z. Li, J. Zhou, Z. Mutlu, M. Sotzing, P. Rajak, S. Shukla, J. Vellek, M. A. Baferani, M. Cakmak, P. Vashishta, R. Ramprasad, Y. Cao and G. Sotzing, *Energy Environ. Sci.*, 2022, **15**, 1307–1314.
- 5 Z. Pan, L. Li, L. Wang, G. Luo, X. Xu, F. Jin, J. Dong, Y. Niu, L. Sun, C. Guo, W. Zhang, Q. Wang and H. Wang, *Adv. Mater.*, 2023, **35**, 2207580.
- 6 G. Liu, Q. Lei, Y. Feng, C. Zhang, T. Zhang, Q. Chen and Q. Chi, *InfoMat*, 2023, **5**, e12368.
- 7 S. Cheng, Y. Zhou, Y. Li, C. Yuan, M. Yang, J. Fu, J. Hu, J. He and Q. Li, *Energy Storage Mater.*, 2021, **42**, 445–453.
- 8 W. Ren, M. Yang, L. Zhou, Y. Fan, S. He, J. Pan, T. Tang, Y. Xiao, C.-W. Nan and Y. Shen, *Adv. Mater.*, 2022, **34**, 2207421.
- 9 Z. Dai, Z. Bao, S. Ding, C. Liu, H. Sun, H. Wang, X. Zhou, Y. Wang, Y. Yin and X. Li, *Adv. Mater.*, 2022, **34**, 2101976.
- 10 T. Zhang, X. Chen, Y. Thakur, B. Lu, Q. Zhang, J. Runt and Q. M. Zhang, *Sci. Adv.*, 2020, **6**, eaax6622.
- 11 B. Zhang, X. Chen, Z. Pan, P. Liu, M. Mao, K. Song, Z. Mao, R. Sun, D. Wang and S. Zhang, *Adv. Funct. Mater.*, 2023, **33**, 2210050.
- 12 M. Feng, Y. Feng, C. Zhang, T. Zhang, X. Tong, Q. Gao, Q. Chen and Q. Chi, *Energy Environ. Mater.*, 2024, **7**, e12571.